Topology-Based Visualization of Time-Dependent 2D Vector Fields

Xavier Tricoche, Gerik Scheuermann, and Hans Hagen

University of Kaiserslautern
P.O. Box 3049, D-67653 Kaiserslautern
Germany
E-mail: {tricoche|scheuer|hagen}@informatik.uni-kl.de

Abstract. Topology-based methods have been successfully applied to the visualization of instantaneous planar vector fields. In this paper, we present the topology-based visualization of time-dependent 2D flows. Our method tracks critical points over time precisely. The detection and classification of bifurcations delivers the topological structure of time dependent vector fields. This offers a general framework for the qualitative analysis and visualization of parameter-dependent 2D vector fields.

1 Introduction

Topology-based visualization of steady 2D vector fields was first introduced by Helman and Hesselink [1]. The location and type identification of the critical points associated with particular streamlines enables a domain partition into subregions where the flow is structurally uniform. This permits a simple, synthetic depiction of vector datasets while preserving the qualitative properties of the flow. This method has been widely applied in the last decade. Yet, in the case of unsteady vector fields, the original method must be extended to offer insight into the qualitative and structural evolution of the 2D flow over time. Helman and Hesselink [2] proposed a solution that consists of computing the topological graph for each given discrete time step. After this, the resulting curves are connected graphically from one time step to the next, based upon qualitative criteria. Here, time is visualized as third dimension. The major drawback of this method is that time is handled in a discrete manner, which prevents the resulting display from identifying and properly depicting the qualitative changes that may occur between two consecutive time steps. As a matter of fact, the introduction of time as an additional parameter has a fundamental consequence: Bifurcations take place that correspond to a transition from a stable structure to another through a punctual unstable state called bifurcation point. Now, the visualization of these features is of major interest because they show how and when a vector field evolves to the structures that are observed on discrete time samples. Their depiction requires the analysis of the vector field as a continuous map defined over a space/time domain.

The paper is structured as follows: First, we briefly review works dealing with the visualization of time-dependent flows. Then we recall fundamental definitions of vector field topology and give an overview of the bifurcation types we have to deal with (section 3). Next, we describe in section 4 how we integrate time in our data structure to get

the required continuous space/time domain. This enables the precise tracking of critical points over time, as explained in section 5. As a last step, the surfaces spanned by the curves of the topological graph must be constructed (see section 6). Results are shown in section 7.

2 Related Work

From the mathematical point of view, the *Visual Math Project* [3] has presented the basic mathematical ideas in an understandable way by the use of discerning sketches. In particular, for depicting bifurcations in 2D, an additional space dimension is used to represent the parameter domain and to visualize the structure evolutions related to it. Furthermore, the practical significance of unsteady flow fields has led to several techniques for the visualization of time-dependent vector fields. In [4], Dickinson has described a method for the interactive analysis of the topology of time-dependent 2D or 3D vector fields. The focus is the correlation of the separatrices between consecutive time steps. This is achieved by solving symbolically the eigensystem of the Jacobian. A method for computing streaklines in 3D unsteady flow fields has been proposed in [5]. The basic principle is to integrate streaklines thanks to an interpolation over space and time. The technique works also with moving grids. Using this scheme, a method for displaying unsteady flow volumes has been presented in [6]. Based upon an adaptive subdivision strategy, the authors arrive at integrating streaklines starting on a generating polygon. For the purpose of feature visualization, in [7], one tracks and correlates the extracted structures by detecting the following fundamental events: Continuation, bifurcation, amalgation, creation and dissipation.

3 Time-Dependent Topology

3.1 Topology

The topology of steady planar vector fields is formed by critical points, some particular streamlines that connect them called separatrices and closed orbits (or cycles) that act as sinks or sources. If one focuses on singularities of first order, there are 5 common types of singularities (see Fig. 1). Note that attracting nodes and foci constitute sinks while

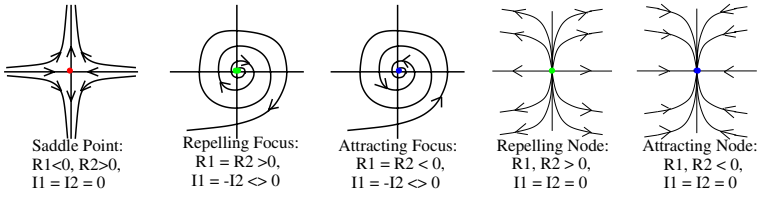

Fig. 1. Common first order singularity types

repelling nodes and foci are sources. A fundamental invariant is the so-called index of a critical point, defined as the number of field rotations while traveling around the critical point along a closed curve, counterclockwise. Note that all sources and sinks mentioned above have index +1 while saddle points have index -1. In a first order approximation, separatrices are defined as those streamlines that start or end at a saddle point.

3.2 Bifurcations

If we turn now to time dependent vector fields, we have to face topological features that are fundamentally new: When the time parameter varies, the qualitative structure of the topology may change from one stable state to another. Such changes are called *bifurcations*. One distinguishes between two types of bifurcations: On one hand, some bifurcations only affect the nature of a singular point or a closed orbit and the corresponding new stable state is to be found in a neighborhood: These bifurcations are called *local bifurcations*. On the other hand, bifurcations that change the global structure of the flow and cannot be deduced from local information are called *global bifurcations*. In the following, we focus on typical 2D local bifurcations and say a few words about global bifurcations.

Local Bifurcations. There are actually two main types of local bifurcations affecting the nature of a singular point in 2D vector fields. The first one is the so-called *Hopf bifurcation* and the second one is the pairwise annihilation or creation of a saddle and a source or sink, called fold bifurcation. Other local bifurcations (like those where an attracting and a repelling closed orbit appear simultaneously for instance) may also occur. Yet, for our purpose, we only pay attention to those that entail a nature transition for a singularity.

Hopf Bifurcation. We start with an attracting focus. If the attracting effect of this sink weakens, the number of streamline rotations around this critical point increases (the convergence "slows down"). This corresponds mathematically to an increasing negative real part of the complex conjugate eigenvalues of the Jacobian matrix at the critical point. When the real part is zero, we get a center point, which is an unstable structure: A bifurcation has occurred. If the real part increases further, a new stable structure appears which consists of an attracting closed orbit typically moving away from the critical point. The critical point itself has transformed into a repelling focus (i.e. a source). So, a sink has changed into a source with the emission of a cycle: This is a Hopf bifurcation. An illustration of this evolution is given in Fig. 2. Inverting the direction of time, we get the transition from a cycle containing a repelling focus into an attracting focus over an instantaneous center. Similar transitions are obtained by inverting the direction of the flow (that is by replacing sources by sinks and vice versa).

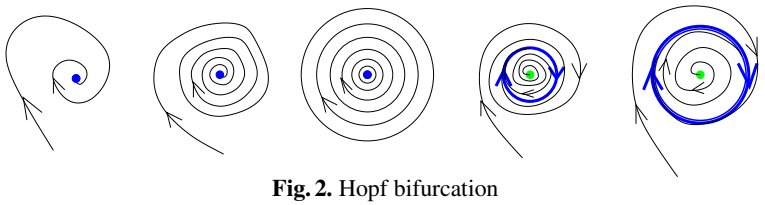

Fig. 2. Hopf bifurcation

Fold Bifurcations. At the beginning, there are a saddle point and a singularity of index +1, say a sink, that are linked by a separatrix. If the attraction/repulsion relation between both singularities along the separatrix weakens (i.e. the real positive eigenvalue of the saddle point, corresponding to the considered separatrix, decreases and the

negative real part of one of both sink's eigenvalues increases), both critical points become closer and closer until they meet. At this point, an unstable critical point appears with a zero eigenvalue: A fold bifurcation has occurred. As time goes on, this unstable structure vanishes: The new stable structure contains no singularity: This is a pairwise annihilation or fold catastrophe (see Fig. 3). Inverting the direction of time, we get a pairwise creation. Similar transitions are obtained by inverting the direction of the flow (the sink becomes a source).

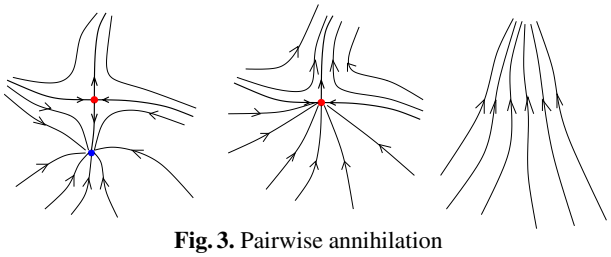

Fig. 3. Pairwise annihilation

Global Bifurcations. As opposed to the cases mentioned above, global bifurcations do not take place in a small neighborhood of a singularity but entail significant changes in the flow structure and involve large domains. We shall not go into details but present an example known as *basin bifurcation*. The essential aspect of such a bifurcation is the saddle/saddle connection as unstable intermediate configuration. If we focus on the basin bifurcation, the situation is as follows. We start with two saddle points that are not connected. This is a stable structure. Progressively, two separatrices become closer and closer until they meet: Both saddle points are connected through this heteroclinic separatrix. This is the bifurcation point. Right after this moment, the separatrix splits into two distinct separatrices which constitutes a swap, compared to the initial configuration.

4 Data Representation

The visualization of time dependent vector data has to deal with a higher dimensional mathematical space where time constitutes an additional dimension. This space must be handled as a continuous one to enable the detection and depiction of fundamental features like bifurcations. In our 2D case, time is considered as third coordinate axis and the whole data is embedded in a 3D scene.

4.1 Grid Construction

Practically, we process a 2D vector field lying on a curvilinear grid with constant positions through time: We dispose the several instantaneous states of the field parallel to another (each of them is called *time plane* in the following), corresponding to their position along the time line. A 3D grid evolves by connecting these planar grids together with 3D cells as shown in Fig. 4(a). There are several possible cell structures for connecting the successive time planes. Since the data points are (in 2D) lying on a

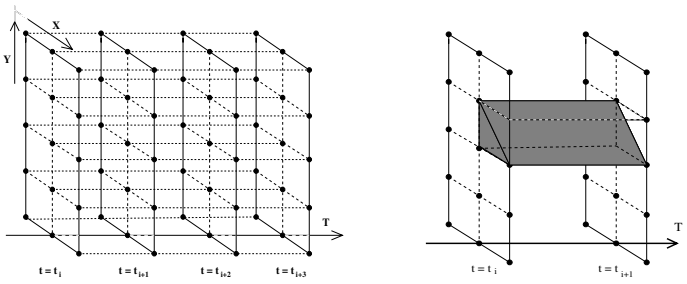

(a) Grid structure (b) Prism cell

Fig. 4. Space/Time grid

structured grid, a natural choice would be to adopt a 3D structured grid made of hexahedron cells. Nevertheless, for the simplicity and efficiency of singularity tracking (see section 5.2), we use prism cells: We first triangulate each time plane and connect the corresponding triangles by translation through time, as in Fig. 4(b). Note that we prefer this cell structure to a simple tetrahedrization of the structured point set because it preserves the structure continuity of each triangle over time.

4.2 Interpolation Scheme

The input data are 2D vectors. Our task consists in interpolating a 2D vector field on a 3D grid. Mathematically, we consider the following map

$$\begin{aligned} f : \mathbb{R}^3 \supset G &\longrightarrow T\mathbb{R}^2 \approx \mathbb{R}^2 \subset \mathbb{R}^3 \\ (x, y, t) &\mapsto \boldsymbol{v}(x, y, t) \equiv (v_1(x, y, t), v_2(x, y, t)) \end{aligned}$$

where G is the 3D grid. Since we need consistency with the piecewise linear interpolation applied on the 2D triangulation, we must ensure that the restriction of the 3D interpolant to each time plane is piecewise linear. This means that if we fix the time coordinate and take it as a parameter, the interpolant must be linear. This is the reason why we choose the following interpolant inside each prism cell.
For a given prism cell lying between $t = t_i$ and $t = t_{i+1}$, let $\boldsymbol{f_j}(x, y) = \boldsymbol{a_j} + \boldsymbol{b_j}x + \boldsymbol{c_j}y$, $j \in \{i, i + 1\}$ be the affin linear interpolants corresponding to the prism triangle faces lying in the planes $\{t = t_i\}$ and $\{t = t_{i+1}\}$ respectively. Then we define the interpolant over the whole prism cell by linear interpolation over time:

$$\boldsymbol{f}(x, y, t) = \boldsymbol{a}(t) + \boldsymbol{b}(t)x + \boldsymbol{c}(t)y$$

where

$$\boldsymbol{a}(t) = \frac{t_{i+1} - t}{t_{i+1} - t_i}\boldsymbol{a}_i + \frac{t - t_i}{t_{i+1} - t_i}\boldsymbol{a}_{i+1}$$

(idem for $\boldsymbol{b}$ and $\boldsymbol{c}$). This formula obviously ensures, for each fixed value t, that $\boldsymbol{f}_t$ is affin linear in x and y.

5 Singularity Tracking

In this section, we track critical points over time, using the interpolation scheme presented above, and seek fold and Hopf bifurcations that may modify the topological structure. To reduce the memory needs of our method, we do not process the whole grid at once: We consider only two consecutive time planes and handle the prism cells connecting them, forming a "time slice".

5.1 Cell Analysis

Singularity Path The interpolant has been chosen so that it contains at most one critical point for a fixed value of t in a cell. This is due to the affin linear nature of its restriction to any time plane. Straightforward calculus leads to the following singularity coordinates $(x(t), y(t))$.

$$\begin{cases} x(t) = |-\boldsymbol{a}(t) \;\; \boldsymbol{c}(t)| \;\; |\boldsymbol{b}(t) \; \boldsymbol{c}(t)|^{-1} \\ y(t) = |\boldsymbol{b}(t) \;\; -\boldsymbol{a}(t)| \;\; |\boldsymbol{b}(t) \; \boldsymbol{c}(t)|^{-1} \end{cases}$$

If t moves from t_i to t_{i+1}, the singularity position describes a 3D curve. Yet, we are only interested in the curve sections that intersect the interior domain of the considered prism cell. A simple way to determine them is to consider the singularities lying on the side faces of the prism: Two triangular faces lying in $t = t_i$ and $t = t_{i+1}$ and 3 quadrilaterals connecting them. Finding the position of a singularity in each prism face requires the solution of a simple linear (resp.quadratic) system. If this is done, we sort the found (3D) positions in ascending time order and associate them pairwise. Indeed, since only one critical point can be present in a prism cell at a given time t, we know that a critical point must first leave the cell before it reenters it later. So, for each pair, we identify an entry and an exit position.

Path Type We now need to pay attention to the singularity types to complete the topological information. The generic types of linear singularities are *source*, *sink* or *saddle* (omitting *center* points that correspond to a transition between source and sink). The transition from one type to another constitutes a bifurcation. In section 3, we have shown that one needs to focus on two bifurcation types and their inverses: fold and Hopf bifurcation. Since a prism cell contains at most one critical point for a given t, we can assert that no fold bifurcation (involving two critical points) can occur inside it: *A fold bifurcation must occur at the cell boundary*. Consequently, we only seek Hopf bifurcations occurring between two consecutive entry and exit points. Practically, the determination of a singularity type is based upon the eigenvalues of the Jacobian at its position. In our case, decomposing the vectors $\boldsymbol{b}$ and $\boldsymbol{c}$ in the canonical basis ($\boldsymbol{b} = b^0\boldsymbol{e_0} + b^1\boldsymbol{e_1}$, idem for $\boldsymbol{c}$), this matrix is

$$J(t) = \begin{pmatrix} b^0(t) & b^1(t) \\ c^0(t) & c^1(t) \end{pmatrix}.$$

Thus we compute the Jacobian matrix and its associated eigenvalues at each entry and exit point and check if they are the same. If this is the case, we can assert that no Hopf bifurcation has occurred since, otherwise, at least two bifurcations have taken

place, which is impossible since our interpolant varies linearly over time. If the type has changed, a Hopf bifurcation is on the way. Because a Hopf bifurcation corresponds to a transition from a repelling to an attracting nature, the instantaneous nature of the intermediate singularity is a center and the trace of the Jacobian is zero at this point, which we use as criterion to determine the exact time location of the bifurcation.

5.2 Tracking

At this stage, every cell knows the successive entry and exit positions of the singular paths through its interior domain, as well as the possible presence of a Hopf bifurcation on the way. Yet, this information is scattered and must be reconnected to offer a global view of the topology evolution over time. A fundamental aspect of this task is to detect and identify the bifurcations that may take place on the faces. They are detected when connecting singular path sections lying in neighbor cells as we show next.

We start in the time plane $\{t = t_i\}$. The restriction of the grid to this plane is a triangulation. In a boolean array, we indicate for each triangle if its corresponding prism must be further inspected or not. If it has to be inspected, we check the information collected during the cell analysis for a path section starting at an entry point located on the considered triangle face. This provides us with an exit point at which the tracking must be proceeded. This exit point can either lie on a side (quadrilateral) face of the prism or on the triangle face lying in $\{t = t_{i+1}\}$. In the latter case, we signify in the boolean array of the next time plane $\{t = t_{i+1}\}$ that this triangle must be further inspected. If the path left the cell at $t^* < t_{i+1}$ (side face), then it entered a neighboring cell at the same time. Back to a 2D representation, we get in time plane $\{t = t^*\}$ a singular point lying on the common edge of both neighboring triangle cells. Due to the discontinuity of the Jacobian matrix through this edge, the singularity may have another type when considered from the other side. This simple argument explains the possible existence of a bifurcation in such cases. Two situations may actually occur.

- There is a simple crossing of a critical point from one cell to another cell where no singularity was present so far. In this case, the type may change but, because of the index invariance, a saddle remains a saddle (index -1). Practically, a source can become a sink and vice versa (both index +1). As mentioned previously, the transition source/sink or sink/source is a Hopf bifurcation. We easily detect it by checking if the type of a source (resp. a sink) path changes after passing the face.
- The second situation corresponds to a merging of two coexisting critical points in neighboring cells on their common face (common edge in 2D). Now, an important property of the piecewise affin linear interpolant over a triangulation is that two neighboring triangles cannot contain two singularities with same index [8] which implies that only 2 singularities with opposite index can merge in that way: A saddle and a source or a saddle and a sink. This type of bifurcation has been considered in section 3: It is a fold bifurcation or its inverse.

When we leave the current cell through a side face, and a possible bifurcation has been detected, we identify this position. We proceed with tracking the path by asking the neighbor cell for the next exit position. We get three possible answers.

1. The exit position lies in the time plane $\{t = t_{i+1}\}$: We have reached the next time plane. The corresponding triangle face is marked `true` in the boolean array corresponding to the next time plane.
2. The "exit" position lies in the time plane $\{t = t_i\}$: If we were tracking the current path forward so far, we have found a pairwise annihilation. In this case, the corresponding triangle is set to `false` in the boolean array of $\{t = t_i\}$, indicating that this cell has been processed now.
3. The exit position lies on a side face for $t = t^{\#}$. If $t^{\#} < t^*$ and we were tracking the current path forward so far, we have found a pairwise annihilation and proceed with backward tracking. If $t^{\#} > t^*$ and we were tracking the current path backward so far, we have found a pairwise creation and proceed with forward tracking: We are back to the current situation.

6 Separating Surfaces

In the 2D steady case, separatrices are curves that emanate from saddle points. Now, as the saddle points move through the 2D/time grid, so do their corresponding separatrices that describe *separating surfaces*. To depict them, we use the information gained about the singular points in the tracking step.
Practically, given a saddle path, we save, at its first position in time and for each of its four separatrices, the following information: Starting vector, associated direction and index of the singular path reached if any or last position obtained by numerical integration and corresponding case: `boundary` (one left the grid) or `cycle` (one reached a closed orbit). At every position along the saddle path, we associate each separatrix with one at the previous position by taking its best approximation in term of starting vector and direction. After that, if both corresponding separatrices reach the same singular path, the same cycle or close positions on the grid boundary, we add the new separatrix to the surface spanned by the old one (we add a new "ribbon" to this surface). Otherwise, we check if the path reached previously has ended at a bifurcation point. In this case, we end the previous surface at the bifurcation by integrating a separatrix at the exact time position of the bifurcation and start a new one at the current separatrix. If no bifurcation has occurred but the connectivity has changed, then we face a global bifurcation that could not be detected while tracking the singularities: We simply end the surface at the previous separatrix and start a new surface at the current separatrix. Doing this for each discrete position along the saddle path, and that for each saddle path, we depict eventually all separating surfaces in the domain.

7 Results

To test our method, we have created an analytic vector field containing four critical points, of which position is a function of time, describing closed curves in the plane. We have sampled this vector field on a rectilinear point set for several values of the time parameter. The rotation of the critical points (each with a specific frequency) entails many structural changes for the topology, which is very interesting for our purpose since bifurcations are present and may be observed with our method. We show first the results of the singularity tracking step: The path of each critical point through time has

been tracked as well as all the local bifurcations taking place (indicated by small balls). The grid is displayed to give an impression (see Fig. 5). If one focuses on a particular bifurcation, one can observe how the separatrices evolve through the bifurcation point. In the case of a Hopf bifurcation for instance, we consider the picture (without surfaces drawn to ease interpretation) in Fig. 6: The creation of a closed orbit can be easily seen. At last, as an illustration of the topological pictures our method can produce, Fig. 7 proposes an overview of the whole topology evolution in the same perspective as in Fig. 5. The breaks that can be observed on the surfaces correspond to structural transitions associated with bifurcations. The two colors used for the surface depiction refer to the stable and unstable directions of the saddle points, respectively.

8 Conclusion

We have presented a topology-based method for the visualization of time-dependent planar vector fields. The topological graph is tracked over time. The interpolation of the discrete planar data over time enables the precise detection of local bifurcations that result in dramatic structural changes. Thus, singularity paths are displayed as well as the bifurcations that affect them. These paths are connected in 3D by separatrix surfaces that provide the structure of the visualized topology.
We think that this technique offers a general framework for the visualization of parameter-dependent planar vector fields.

References

[1] Helman J.L., Hesselink L., *Representation and Display of Vector Field Topology in Fluid Flow Data Sets*. Visualization in Scientific Computing, G.M. Nielson & B. Shriver, eds., 1989.

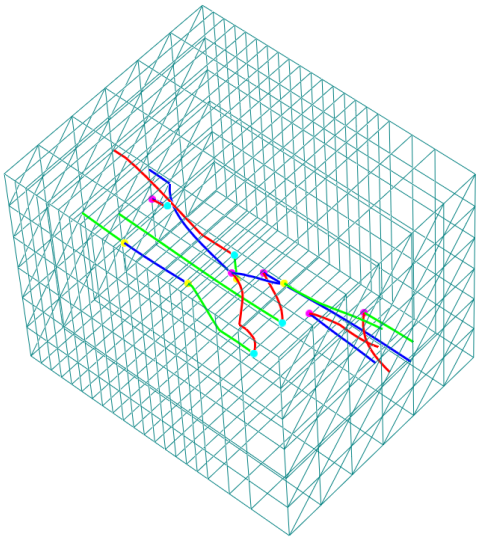

Fig. 5. Singular paths and bifurcations

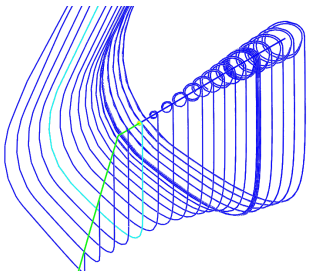

Fig. 6. Hopf bifurcation (lines)

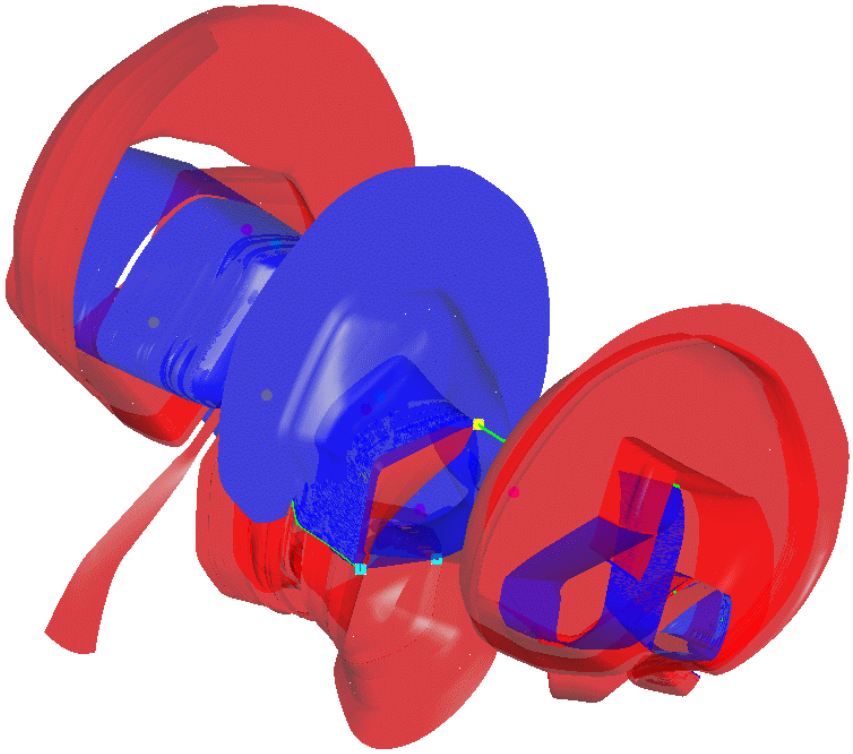

Fig. 7. Overview of the topology evolution

[2] Helman J.L., Hesselink L., *Surface Representation of Two- and Three-Dimensional Fluid Flow Topology*. Proceedings of the First IEEE Conference on Visualization, pp.6-13, IEEE Computer Society Press, Los Alamitos CA, 1990.

[3] Abraham R.H., Shaw C.D., *Dynamics The Geometry of Behavior, Part I-IV*. Aerial Press, Santa Cruz, CA, 1982-1988.

[4] R.R. Dickinson *Interactive Analysis of the Topology of 4D Vector Fields*. IBM Journal of Research and Development, Vol. 35, No. 1/2, January/March 1991.

[5] Lane D.A., *UFAT - A Particle Tracer for Time-Dependent Flow Fields*. Proceedings IEEE Visualization'94, IEEE Computer Society Press, Los Alamitos CA, 1994.

[6] Becker B.G., Lane D.A., Max N.L., *Unsteady Flow Volumes*. Proceedings IEEE Visualization'95, IEEE Computer Society Press, Los Alamitos CA, 1995.

[7] Silver D., *Feature Visualization* In Scientific Visualization Overviews - Methodologies - Techniques, pp.279-293, G.M. Nielson, H. Hagen, H. Müller (eds.), IEEE Computer Society, Los Alamitos CA, 1997.

[8] Scheuermann G., Hagen H., *A Data Dependent Triangulation for Vector Fields*. In proceedings of Computer Graphics International 1998, pp.96-102, F.-E. Wolter, N. M. Patrikalakis (eds.), IEEE Computer Society Press, Los Alamitos CA, 1998.